An Experimental Study on the Temperature Distribution in IRWST

Sang-Nyung Kim*
Department of Nuclear Engineering, Kyunghee University Seocheon-ri #1, Kiheung-up, Youngin-city, Kyung-ggi-do 449-701, Korea

The In-Containment Refueling Water Storage Tank (IRWST), one of the design improvements applied to the APR-1400, has a function to condense the high enthalpy fluid discharged from the Reactor Coolant System (RCS). The condensation of discharged fluid by the tank water drives the tank temperature high and causes oscillatory condensation. Also if the tank cooling water temperature approaches the saturated state, the steam bubble may escape from the water uncondensed. These oscillatory condensation and bubble escape would burden the undue load to the tank structure, pressurize the tank, and degrade its intended function. For these reasons simple analytical modeling and experimental works were performed in order to predict exact tank temperature distribution and to find the effective cooling method to keep the tank temperature below the bubble escape limit (93.3℃), which was experimentally proven by other researchers. Both the analytical model and experimental results show that the temperature distributions are horizontally stratified. Particularly, the hot liquid produced by the condensation around the sparger holes goes up straight like a thermal plume. Also, the momentum of the discharged fluid is not so strong to interrupt this horizontal thermal stratification significantly. Therefore the layout and shape of sparger is not so important as long as the location of the sparger hole is sufficiently close to the bottom of the tank. Finally, for the effective tank cooling it is recommended that the locations of the discharge and intake lines of the cooling system be cautiously selected considering the temperature distribution, the water level change, and the cooling effectiveness.

Key Words : APR-1400, SDS, IRWST Temperature Distribution, Bubble Escape Temperature, Thermal Stratification

Nomenclature

A : Area
C_p : Heat capacity of water
g : Gravity acceleration
g_c : Constant of proportionality
Gr : Grashof number
K : Flow coefficient
L : Submerged depth
$\dot{m}$: Mass flow rate
M : Mass of water
ΔP : Pressure drop
T_w : Limit temperature of water
T : Tank temperature far from the sparger
Y : Expansion factor
r : Radius of condensation front

Greeks

β : Thermal expansion coefficient of water
v : Velocity
ρ : Density

Subscript

b : Bottom
t : Top

* **E-mail** : snkim@khu.ac.kr
TEL : +82-31-201-2561; **FAX** : +82-31-202-1541
Department of Nuclear Engineering, Kyunghee University Seocheon-ri #1, Kiheung-up, Youngin-city, Kyung-ggi-do 449-701, Korea. (Manuscript **Received** February 10, 2003; **Revised** February 9, 2004)

a : Average
c : Condensation
h : Hot plume
o : Orifice
s : Steam
∞ : Liquid far from the sparger hole
l : Liquid
f : Saturation
T : Tank

Abbreviations

IRWST : In-Containment Refueling Water Storage Tank
APR : Advanced Pressurized Reactor
RCS : Reactor Coolant System
PSV : Pressurizer Safety Valve
SDS : Safety Depressurization System
RHRS : Residual Heat Removal System

1. Introduction

The IRWST, one of the design improvements applied to APR-1400, is a Refueling Water Storage Tank (RWST) installed inside the containment. By introduction of this system, the reliability of the safety injection system and containment spray system can be enhanced since the IRWST can omit the operator of actions to switch the injection mode into the recirculation mode in a transient (or an accident). On actuating the Pressurizer Safety Valve (PSV) or Safety Depressurization Valve (SDV), the IRWST also prevents the containment from being contaminated by the discharged high radioactive steam. Due to this function, without the burden of decontamination cost, the operator can make quick decision whether the Safety Depressurization System (SDS) be actuated or not. Finally in severe accidents, the IRWST may provide the reactor cavity with the tank coolant. The provided water can cool the outside of the reactor vessel or capture/cool the discharged molten core. Therefore, the integrity of the containment must be maintained by preventing the reactor vessel penetration and direct containment heating caused by the molten core may be prevented (Kyungho et al., 1996 ; Heoyjung, 1996 ; Korean Next Generation Reactor, Center for Advanced Reactor Research, 1994).

To ensure the above mentioned functions for all kinds of plant transients, the most severe transient case should be identified and analyzed. The most-limited thermal transient for the IRWST is the total loss of feedwater event with the feed and breed operation. In this case, the temperature of the cooling tank is supposed not to exceed 93.3℃ (Korea Atomic Energy Research Institute, 1994 ; KEPCO, 1994 ; Combustion Engineering, 1994). The temperature limit is imposed to protect the system from the severe condensation oscillation by the discharged steam, and prevent the discharged steam from escaping uncondensed and pressurizing the tank.

The limit condition may have some margin if the total water inventory of the tank contributes uniformly to the condensation of the discharged fluid. However, the water away from steam discharging pipes (spargers) contributes less to the steam condensation and the water around spargers contributes more since spargers are nonuniformly distributed over the inside of the annular space of IRWST. Also the tank can be thermally stratified by the hot plume of condensed water. Due to this geometrical nonuniform location of the spargers and thermal stratification the temperature limit can be exceeded locally around the sparger for some transients. To suppress this local temperature peaking below the limit, the circulation of water through the Residual Heat Removal System (RHRS) is considered (Combustion Engineering, 1994 ; KOPEC, 1996). Therefore, this study aims at the experimental prediction of the temperature distribution and the effective cooling method to keep the temperature below the limit (Lubin, 1991).

2. Thermal Stratification

The steam discharged from the sparger is condensed by the cold tank water around the sparger. The condensed water has thermal buoyancy due to its hot temperature. The hot steam discharged from the sparger is condensed not far from the sparger hole. Except the transient situation such as air and steam clearing period, the condensation front are very stable. This means that the horizontal momentum of the discharged hot steam jet is overcome by the opposite horizontal direction momentum of the incoming cold water. The discharged hot jet contribute to the vertical thermal buoyancy only. Therefore the hot water goes up almost straight around the sparger. When the upward hot water reaches at the free surface, the water flows horizontal and radially. This hot water forms thermal stratification. The fluctuation pressure due to condensation can not distrupt this thermal stratification. This assertion can be verified by simple analytical model and experiment.

By the assumption of semispherical condensation front, the conservation equations for the control volume of uniform condensation over the front can be derived as follows (See Figure 1).

Mass Conservation Equation

$$\dot{m}_h = \dot{m}_s + \dot{m}_c \tag{1}$$

$$\dot{m}_c = 2\pi\rho_\infty v_c r^2 \tag{2}$$

Momentum Conservation Equation (Horizontal direction)

$$\Sigma\vec{F} = \underbrace{\frac{\partial}{\partial t}\int_{c,v}\rho\vec{V}dV}_{0\ \text{steady}} + \int_{c,v}\rho\vec{V}\vec{V}\cdot d\vec{A} \tag{3}$$

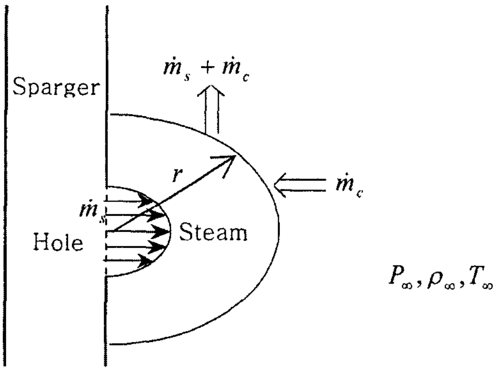

Fig. 1 Control volume for the thermal stratification

$$\Sigma\vec{F} = \underbrace{\Sigma F_{shear}}_{\text{No shear}} + \underbrace{\Sigma F_{pressure}}_{\text{No variation}} = 0 \tag{4}$$

$$\frac{1}{2}\pi r^2\rho_\infty v_c^2 \cdot = \rho_s v_s^2 \cdot A_s \tag{5}$$

$$2\pi r^2\rho_\infty v_c^2 \cdot = \dot{m}_c v_c = 4\dot{m}_s v_s \tag{6}$$

$$v_c = \frac{4\dot{m}_s v_s}{\dot{m}_c} \tag{7}$$

The pressure force in eq. (4) is negligible since in the semispherical model, steamline of the steam flow is straight so that the pressure variation across the flow is zero. That means the pressure at the hole is same at that far from the hole.

Energy Conservation Equation

$$\dot{m}_c(h_f - h_\infty) = \dot{m}_s(h_s - h_f) \tag{8}$$

$$\therefore\ \dot{m}_c = \dot{m}_s\frac{(h_s - h_f)}{(h_f - h_\infty)} \tag{9}$$

$$v_c = \frac{4\rho_s v_s^2 A_s}{\dot{m}_s\left(\frac{h_s - h_f}{h_f - h_\infty}\right)} = 4\frac{\dot{m}_s}{d\dot{m}_c}v_s = 4v_s\left(\frac{h_f - h_\infty}{h_s - h_f}\right) \tag{10}$$

$$r = \sqrt{\frac{\dot{m}_c}{2\pi\rho_\infty v_c}} = \left(\frac{h_s - h_f}{h_f - h_\infty}\right)\sqrt{\frac{\dot{m}_s}{8\pi\rho_\infty v_s}} = \left(\frac{h_s - h_f}{h_f - h_\infty}\right)\sqrt{\frac{\rho_s A_s}{8\pi\rho_\infty}} \tag{11}$$

For the experiment condition, the calculated value are tabulated in Table 1.

The condensation front radius is calculated to be very small so that the condensation is accomplished at the just hole front.

Also the temperature distribution of the liquid in the tank can reasonably be predicted by a following simple analytical model. The model is based on the following assumptions.

(1) The hot condensate goes up straight to the liquid surface and stratified from the top surface.

(2) The rising time of the hot condensate is very short compared to the whole transient time.

Table 1 Experimental condition

	v_s(m/sec)	$\dot{m}_c$(kg/sec)	v_c(m/sec)	r(m)	Remarks
Calculated value	196.7	0.0453	109.5	2.6×10^{-4}	$\dot{m}_s$(per hole) $=0.02535$ kg/sec $A_s=3.904\times10^{-5}$ m^2 $\rho_s=2.549$ kg/m^3

(3) The discharged steam mass is negligible compared to the whole liquid mass in the tank.

(4) The steam flow rate is constant.

(5) When some time passed after the start of steam discharge, the temperature difference between the top and bottom of the tank is almost constant.

Then, during the time interval dt, the energy balance of the tank for the steam and the tank liquid is following.

$$\begin{aligned} &\dot{m}_S h_S dt + M_T C_P T_a \\ &= (\dot{m}_S dt + M_T)\, C_P (T_a + dT_a) \end{aligned} \tag{12}$$

and $C_P T_a = h_C$

$$\dot{m}_S (h_S - h_C) \approx M_T C_P \frac{dT_a}{dt} \tag{13}$$

The temperature difference between the top and bottom of the tank ΔT is $(T_t - T_b)$, and $T_a = \frac{1}{2}(T_b + T_t) = T_b + \frac{1}{2}\Delta T$. Therefore,

$$\begin{aligned} \frac{dT_a}{dt} = \frac{dT_b}{dt} &= \frac{\dot{m}_S (h_S - h_C)}{M_T C_P} \\ &= \frac{\dot{m}_S \left(h_b - \frac{1}{2} C_P \Delta T \right)}{M_T C_P} \end{aligned} \tag{14}$$

and finally, the equation (11) is reduced to the following because $h_S \gg \frac{1}{2}\Delta T C_P$

$$\frac{dT_b}{dt} + \frac{\dot{m}_S}{M_T} T_b \approx \frac{\dot{m}_S}{M_T C_P} h_S \tag{15}$$

The solution of this first order inhomogeneous equation with an initial condition, $T_b = T_b(0)$ at time $t = 0$.

$$T_b(t) = \frac{h_S}{C_P}\left(1 - e^{-\frac{\dot{m}_s}{M_T} t}\right) + T_b(0)\, e^{-\frac{\dot{m}_s}{M_T} t} \tag{16}$$

Therefore, the temperature of the tank surface (highest liquid temperature) is predicted as follow.

$$\begin{aligned} T_t(t) &= \Delta T(t) + T_b(t) \\ &= T_t(0) - T_b(0) + \frac{h_S}{C_P}\left(1 - e^{-\frac{\dot{m}_s}{M_T} t}\right) \\ &\quad + T_b(0)\, e^{-\frac{\dot{m}_s}{M_T} t} \end{aligned} \tag{17}$$

where, $\frac{\dot{m}_S}{M_T} \approx 0$, $\Delta T(t) = \Delta T(0) = T_t(0) - T_b(0)$

$$\begin{aligned} T_t(t) &\approx T_t(0) - T_b(0) + \frac{h_S}{C_P}\left(1 - 1 + \frac{\dot{m}_S}{M_T} t\right) \\ &\quad + T_b(0)\left(1 - \frac{\dot{m}_S}{M_T} t\right) \\ &= T_t(0) + \frac{h_S}{C_P}\frac{\dot{m}_S}{M_T} t - T_b(0)\frac{\dot{m}_S}{M_T} t \\ \text{or } &= T_t(0) + \left[\frac{h_S}{C_P} - T_b(0)\right]\frac{\dot{m}_S}{M_T} t \\ &= \Delta T + T_b(0) + \left[\frac{h_S}{C_P} - T_b(0)\right]\frac{\dot{m}_S}{M_T} t \end{aligned} \tag{18}$$

3. Experimental Facility

The experimental facility consists of a water tank (IRWST), a steam generator, a sparger, and some instrumentations (such as thermocouples, a flow meter, a level gage, and a pressure gage, etc.). A water level gauge, a thermometer (0~300℃), a safety valve, and a pressure gauge (0~1 MPa) are installed on the steam generator as shown in Fig. 2. The tank has 75 cm ID, 125 cm height, and its design pressure is 0.19 MPa.

3.1 The modeling of IRWST

The IRWST of APR-1400 is a 3.66 m (12 ft) deep annular water tank (Lubin, 1991 ; Park, 1996). The spargers are vertically submerged and each has a hole at the bottom end. The water depth to the lowest hole is 1.98 m. The submerged depth of the model sparger is determined by the Grashof number which is a most important dimensionless parameter that governs the thermal stratification and natural circulation in the tank. In the calculation of the Grashof number, it can be defined as (Bae et al., 2002,).

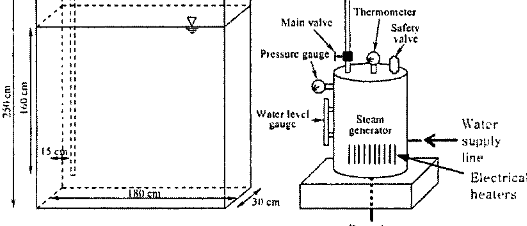

Fig. 2 Schematic diagram of the experimental facility

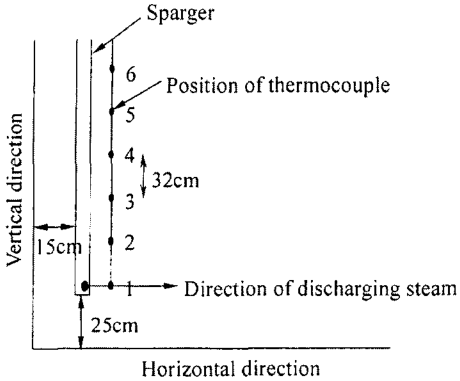

Fig. 3 Schematic diagram of sparger and positions of T/C

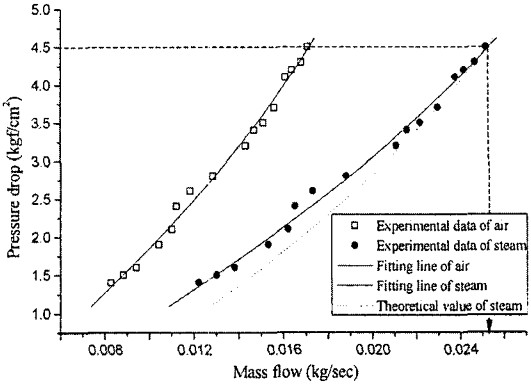

Fig. 4 The flow rate comparison between the calibrated and correlation

$$Gr = \frac{g\beta(T_w - T_\infty)L^3}{r^2} \quad (19)$$

The peak temperature of the IRWST and ambient temperature of the pool water were assumed 100℃ and 25℃, respectively. The submerged depth of the model sparger is calculated from the relation as follows.

$$Gr_{prototype} = Gr_{model} \quad (20)$$

For a model, the submerged depth of the sparger is 160 cm and the IRWST is the rectangular tank of 250 cm high, 30 cm wide and 180 cm long as shown in Fig. 2.

An I type sparger with 4 holes around the pipe was installed to be discharge the steam horizontally. Each hole is 4 mm in diameter and 90 each other. The size and number of the hole were determined to simulate the mass flux effect of the discharged steam (See Figure 3).

3.2 Mass flow rate

The mass flow rate was measured by a flow meter consisted of a orifice and a pressure transducer (with the limits of error $\pm 0.75\%$). As shown in Fig. 4, the steam flow meter was calibrated by air flow rate. The air flow rate was measured by the water replacement method as follows.

The air blown by a compressor was forced to flow though the flowmeter and then the air collected by the mass cylinder under water for a presetted time. During the time the pressure drop across the meter was measured. Then the steam flow rate was reduced as follow (Robert P. Benedict, 1977).

$$\Delta P = \frac{1}{2}\rho_{air}u_{air}^2 = \frac{1}{2}\rho_{steam}u_{steam}^2 \quad (21)$$

$$u_{air} = \frac{\dot{m}_{air}}{\rho_{air}A_o},\ u_{steam} = \frac{\dot{m}_{steam}}{\rho_{steam}A_o} \quad (22)$$

$$\dot{m}_{steam} = \sqrt{\frac{\rho_{steam}}{\rho_{air}}}\,\dot{m}_{air} \quad (23)$$

where

$\dot{m}_{air} = \rho_{air} V_{air}/time$

$V_{air} = 0.15\ m^3$ (measured air volume)

$\rho_{air}(27℃) = 1.176\ kg/m^3$

$\rho_{steam}(150℃) = 2.549\ kg/m^3$

The calibrated result is compared with the correlation (Holman, 1989) (See Figure 4).

For orifices, the correlation is defined as follows :

$$\dot{m}_{air} = KYA_o\sqrt{2\rho_{air}\Delta\rho} = 1.72\times10^{-2}\ kg/sec \quad (24)$$

where

$K = 0.6098$

$Y = 0.7092$

$A_o = 3.904\times10^{-5}\ m^2$

$\Delta P = 441.3\ kPa$

The constant steam flow rate 0.0252 kg/sec, is steadily controlled by a discharge valve and the

Table 2 Experimental matrix

	Part 1	Part 2	Part 3
Interested Region	Around the sparger hole and along the sparger pipe	Half tank	Extended whole tank
Experiment Purpose	Detailed temperature distribution around the sparger pipe	Vertical and horizontal temperature distribution in the tank	Temperature distribution in extended tank (Tank size effect)
Dimension	One dimension (Diameter 2 cm × 160 cm)	Two dimensions (80 cm × 160 cm)	Two dimensions (160 cm × 160 cm)
Thermocouple Array	6×4	6×14	6×24

constant heat inputs through a 71 kW steam generator. The maximum steam mass flux, 500 kg/s·m^2, at the sparger hole is determined so that the mass flux and ΔT_{sub} can be covered the whole range of the typical IRWST condensation map. To satisfy these conditions, the hole size and number of hole have been determined to be adequate to the heater capacity.

The temperature is measured by K-type thermocouples precalibrated with IPRC (Ice Point Reference Chamber) and insulated by lac coating. The K-type thermocouple has 0.75% above 0℃ and 2% below 0℃ in the limits of error. The thermocouple array is consisted of 6 in a column and 4 in a row as shown in Fig. 3. The temperature signals through a rotary multichannel selector are processed by a multimeter.

4. Experimental Works

4.1 Experimental conditions

The experiments were performed as following conditions.

(1) The steam generating tank was operated at 4.7 atm (150℃).

(2) The steam condition at the sparger hole was saturated steam at 0.2 MP(T_f=120℃).

(3) The IRWST pool water temperature was initially 25℃.

(4) The total experimental time was 30 minutes.

(5) If the steam generator reached saturated state, the steam was vented enough to expel all most of the non-condensible gas in the tank through the vent valve.

(6) The fixed flow rate of saturated steam was discharged from the steam generating tank to the IRWST.

(7) The temperatures were measured every 5 minutes.

(8) The temperature distribution was mapped. (Fig. 5, 6 and 9)

4.2 Experiments

The experiments are divided into three parts. The first one (part 1) is intended to find the detailed temperature distribution around the sparger hole and along the sparger, the second one (part 2) to determine the general temperature distribution in the whole tank, and the last one (part 3) to check the horizontal tank size effect. The experiments can be summarized as Table 2.

5. Results and Discussion

5.1 Part 1 experiment

The temperature was measured in the near (1 mm from the pipe) cylindrical region around the sparger hole and along the sparger pipe of diameter 2 cm × 160 cm high.

As shown in Fig. 5, the condensed hot water goes up straight along the sparger pipe except the sparger hole region (Lee et al., 2003). In the sparger hole region, the temperature is almost saturated. As the hot water goes up, the hot water mixes with the around cold water and the temperature drops.

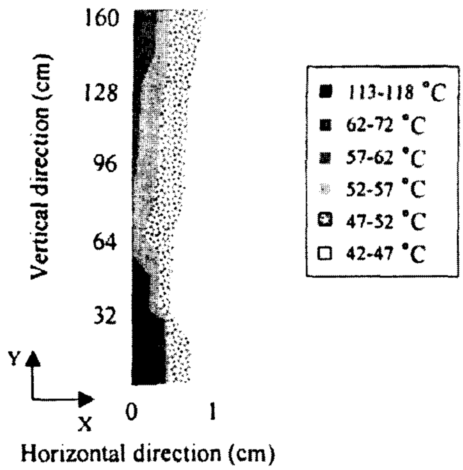

Fig. 5 Temperature distribution in the core region after 30 minutes (Part 1)

However, at the free surface, the hot water spreads horizontally. The thermal mixing range of the hot plume is less than 1 cm from the pipe in the experiment.

5.2 Part 2 experiment

The temperature was measured vertically and horizontally by thermocouples installed at 6×14 points. The horizontal distribution shows no typical characteristics. However, as shown in Fig. 6, the vertical distribution shows mentionable characteristics. These are the thermal stratification which is caused by the buoyant force of hot water. The condensed hot water goes up straight and spreads along the free surface until it reaches the wall of the tank. The hot water then accumulates horizontally. This thermal stratification is more prominent in the Fig. 8 which represents the average temperature distribution.

Also, you can see two thermal islands on the top of the free surface in the right and left corner of Fig. 6 and Fig. 7. The left side island is formed by the hot water just risen from the sparger hole while the right side island is formed by the accumulated hot water at the tank wall.

As expected in the preliminary analysis of the IRWST water temperature distribution, the bulk temperature rises up as the amount of hot steam input increases.

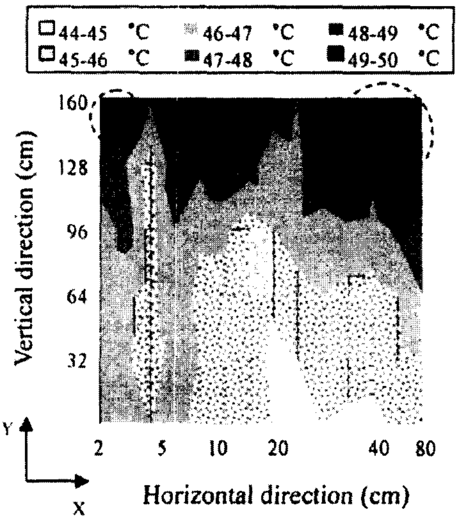

Fig. 6 Temperature distribution in the main region after 30 minutes (Part 2)

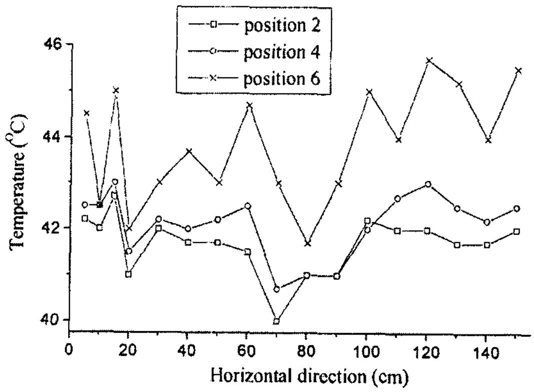

Fig. 7 Horizontal temperature distribution after 30 minutes

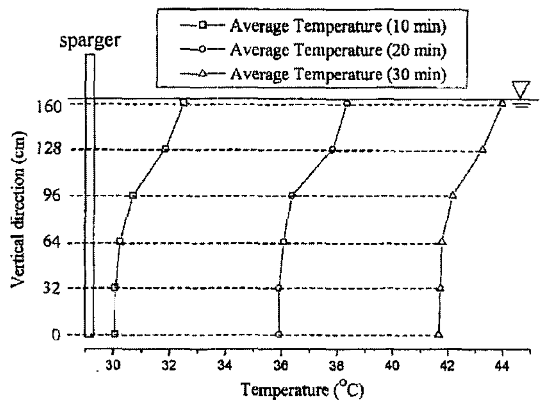

Fig. 8 Vertical temperature distribution

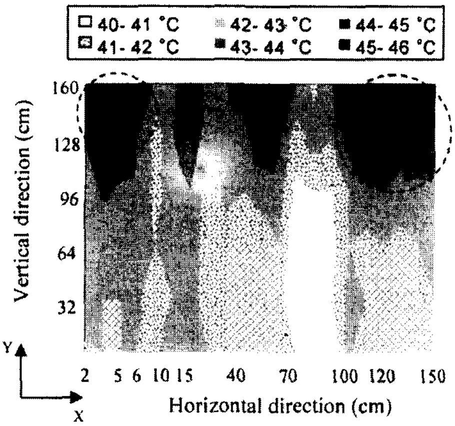

Fig. 9 Temperature distribution in the main region after 30 minutes (Part 3)

5.3 Part 3 experiment

The part 3 experiment was necessary to check the length effect of the tank since the location of the sparger of APR-1400 IRWST are asymmetric.

The horizontal length of the tank was simply extended twice from the 90 cm to 180 cm. As shown in Fig. 9, the condensation occurs efficiently and the hot liquid produced by the condensation around the sparger hole goes up to the surface. The thermal stratification by the thermal plume is also formed as in the part 2 experiment. The horizontal temperature profile has been enlarged along the whole tank length. That means the thermal stratification are valid along the whole tank length.

5.4 Discussion

In the preliminary analysis of the IRWST water temperature distribution and thermal hydraulic loads, the APR-1400 IRWST bulk temperature was, by assuming 100% mixing, estimated to reach the limit temperature of 93.3℃ in 4500 seconds after the steam discharges into the IRWST pool (KOPEC, 1996). In experimental case, the bulk temperature increases linearly and it is presumed to reach the limit temperature of 93.3℃ in about 4800 seconds. For the Total Loss Of Feedwater (TLOFW) event, the full depressurization time is 6000 seconds. Therefore, the cooling system is indispensable to satisfy temperature limit. Also it is recommended

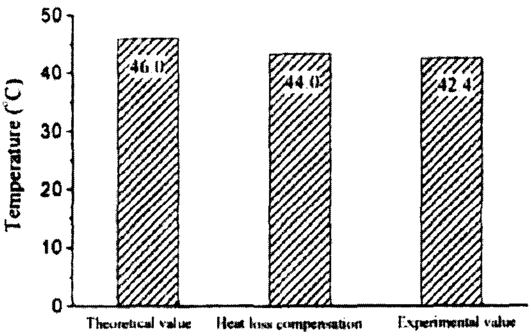

Fig. 10 Comparison between the theoretical and experimental value for average temperature

that the locations of intake and discharge of the cooling system be cautiously selected by considering the temperature distribution, the water level change and the cooling effectiveness. This cooling system can suppress the tank temperature below the limit temperature (93.3℃) up to the end of the depressurization of Reactor Coolant System (RCS).

As shown in Fig. 10, theoretical average temperature of the tank was calculated 46.0℃ by the energy balance between the steam discharged from the sparger holes and the sensible heat of tank water. However, the average temperature of the tank from the experimental result was 42.4℃. The discrepancy may be resulted from the heat losses by convection at the tank wall and the evaporation from the free surface, the heat capacity of tank material, and some errors of measurement and average temperature calculation. The heat losses due to the convection at the wall and the tank material were calculated about 387 kJ and 5180 kJ, respectively. As shown in Fig. 10, these are equivalent to temperature rise of tank water about 0.2℃ and 1.4℃, respectively. The heat loss due to the evaporation and the errors can not figure out specifically. There may be some error in steam flow rate measurement. The error may be resulted from the condensed moisture in the upstream of flowmeter. The moisture can effect pressure drop in the flowmeter.

Also the temperature limit will reach more earlier than expected because of the thermal stratification shown by analytical model and experimental results. The analytical model predicted the top surface temperature increase 30.8℃ during 30 minutes. However the experimental results show that temperature increase is only about 21℃. This discrepancy can be resulted from the model defect, error of measurement and heat loss the tank. The initial tank temperature was uniformly 25℃. Therefore the temperature distribution is not same as the model which the initial temperature was assumed linear.

6. Conclusions

This study has been performed for the development of the prediction method of the temperature distribution and the effective cooling method to keep the temperature below the limit. From this study, the experimental result informs us many important things to the IRWST design. By the simulation experiment of the APR-1400 IRWST, the following conclusions are drawn.

(1) The shape of the sparger is not so crucial since the thermal stratification effect dominates the temperature distribution (Cho and Song, 2001).

(2) If the common engineering sense is employed, the symmetry or the distance between the sparger is not important in the view of the temperature distribution.

(3) The free surface temperature may be set as the limit temperature below which the tank temperature should be kept since the temperature is the highest in the tank except the region around the sparger hole.

(4) The locations of inlet and outlet of the cooling system should be selected by not only considering temperature distribution but by considering the water level change. The temperature difference along the vertical distance is not so much as anticipated.

(5) The tank can be pressurized faster than expected since the tank surface temperature is the highest in the tank except around the sparger hole. The hot water of the free surface can contribute to the build-up of vapor pressure of the tank and the air pressure by heating up the air in the tank atmosphere.

The last thing that should be mentioned is that the experiment was performed only for a limited range. That is, the tank temperature rise is only about 20℃. The limitation of the temperature rise is due to the limit of the boiler capacity. However, the limitation would not significantly affect the experimental result since the temperature profile would not be changed significantly by the temperature rise.

However, to assure the more accurate prediction, further experiments should be executed to accommodate the increase of mass flow and some changes of sparger shape (due to design change).

Acknowledgment

This work is supported by the Korea Science and Engineering Foundation through Center for Advanced Reactor Research (CARR), and Nuclear Power Plant Technology Research Center.

References

Cho, S. and Song, C. H., 2001, "Multiple-Hole Effect on the Performance of a Sparger During Direct Contact Condensation of Steam," *KSME International Journal*, Vol. 15, No. 4.

Choong-Won Lee, Su-Yeon Moon, Chang-Hyun Sohn and Hyun-Jin Youn, 2003, "Spray and Combustion Characteristics of a Dump-type Ramjet Combustor," *Int. Jr.*, Vol. 17, No. 12, pp. 2019~2026.

Combustion Engineering, 1994, "System 80+ Standard Safety Analysis Report Design Certification," Amendment W.

Heoyjung Kim, 1996, "Safety Requirement in KNGR," KINS.

Holman, J. P., 1989, *Experimental Method for Engineers*, Fifth Edition, McGraw-Hill, pp. 231~241.

KEPCO, 1994, "Elementary Requirement in KNGR."

KOPEC, 1996, "IRWST T/H Load Analysis," KOPEC, Korea.

Kangyoul Bae, Hanshik Chung and Hyomin Jeong, 2002, "Convective Heat Transfer in Ventilated Space with Various Partitions," *KSME Int. Jr.*, Vol. 16, No. 5, pp. 676~682.

Koo-Woun Park, Se-Won Lee, Hee-Jin Ko and Young-Sik Jang, 1997, "IRWST Hydrodynamic Loads in KNGR," KOPEC, Korea.

Korea Atomic Energy Research Institute, 1994, "Joint Passive Safety Evaluation Program for System 80+,"

Korean Next Generation Reactor, Center for Advanced Reactor Research, 1994, "Design Concept — The Total Plant Design (IV),"

Kyungho Nam, Hejeon Ko and Jaeyoung Lim, 1996, "IRWST System Design in KNGR," *Power Engineering*, Vol. 7. No. 2, KOPEC.

Lubin, B. T., 1991, "Evaluation of the System 80+ Steam Relief System and IRWST Design."

Robert P. Benedict, 1977, *Fundamentals of Temperature, Pressure and Flow Measurements*, Wiley, pp. 443~469.

Sangdeuk Park, 1996, "Design Requirements and Features of Korean Next Generation Reactor, Center for Advanced Reactor Research of KEPRI," Korea.